

Supplementary Information

Controlling PEDOT:PSS electropolymerization for label-free optical recording of bioelectric potentials

Xuchen Ren^{1†}, Jitong Ren^{2†}, Yu Shi³, Alexandra Kuhlman-Schneider¹, Koney Eungkon Kim¹, Zixin Zhang¹, Yuecheng Peter Zhou^{1,2,4,5,6*}

¹ Department of Materials Science and Engineering, The Grainger College of Engineering, University of Illinois Urbana-Champaign, Urbana, IL, USA.

² Department of Chemical and Biomolecular Engineering, College of Liberal Arts & Sciences, University of Illinois Urbana-Champaign, Urbana, IL, USA.

³ Department of Chemistry, College of Liberal Arts & Sciences, University of Illinois Urbana-Champaign, Urbana, IL, USA.

⁴ Department of Bioengineering, The Grainger College of Engineering, University of Illinois Urbana-Champaign, Urbana, IL, USA.

⁵ Materials Research Laboratory, University of Illinois Urbana-Champaign, Urbana, IL, USA.

⁶ Beckman Institute for Advanced Science and Technology, University of Illinois Urbana-Champaign, Urbana, IL, USA.

† Equal contributions

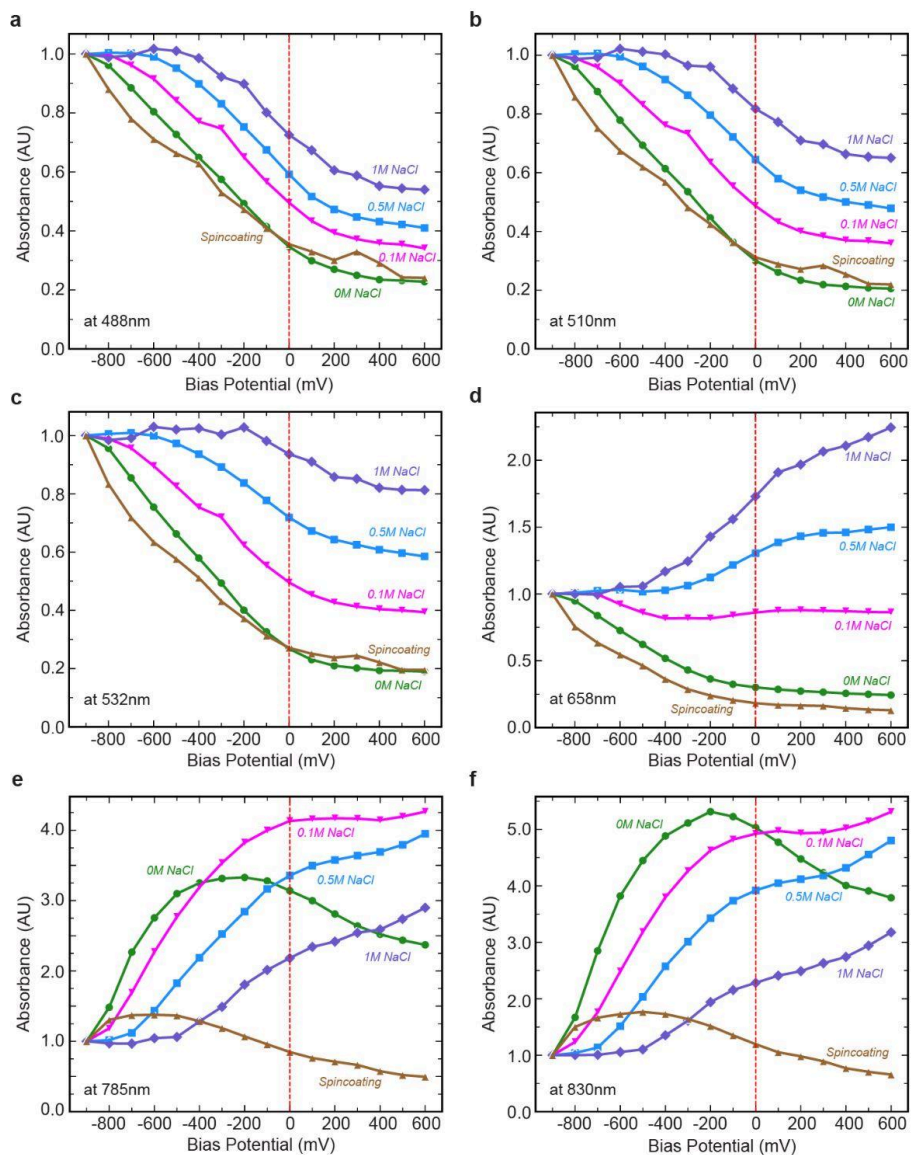
* To whom correspondence may be addressed. Email: zhou62@illinois.edu

Supplementary Text

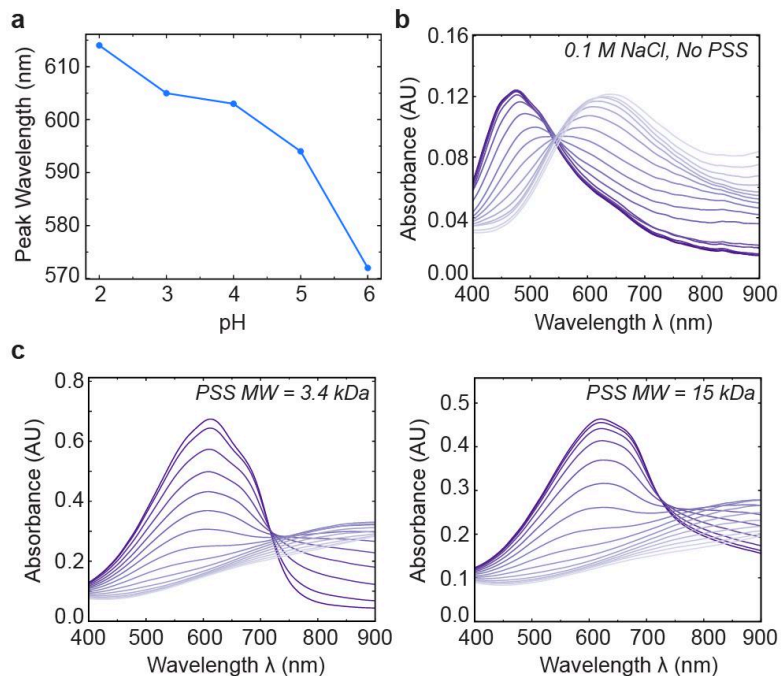
1. Surface treatment of indium tin oxide (ITO)-coated glass

The surface morphology of ITO glass using different surface treatment methods was characterized by atomic force microscopy (AFM) (**Supplementary Figure 3a**). Untreated clean ITO glass (dish soap water, acetone, isopropyl alcohol) exhibits relatively smooth surfaces (RMS roughness of ~0.6 nm) and largest grain size. UV-Ozone treatment leads to slightly reduced grain size but an increased RMS roughness of ~0.8 nm. Oxygen plasma treatment results in a more fragmented surface morphology with the smallest grain size but highest RMS roughness of ~1.0 nm. Details of ITO glass treatments before electropolymerization are described in the Methods section.

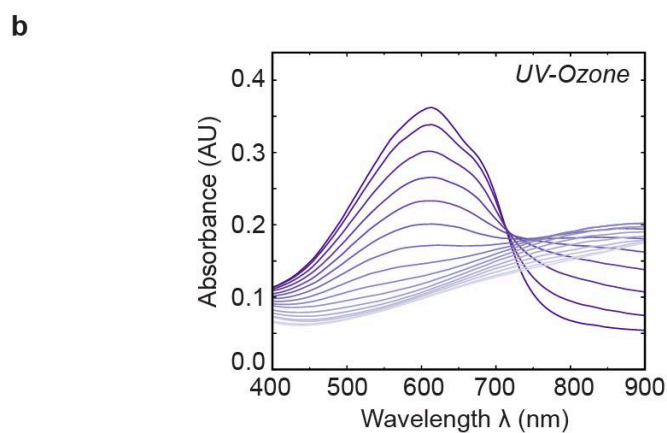
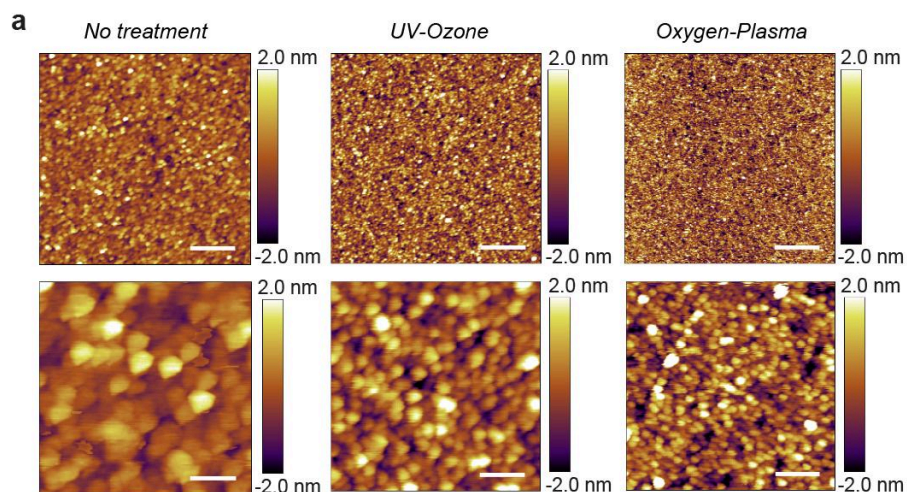
Supplementary Figures



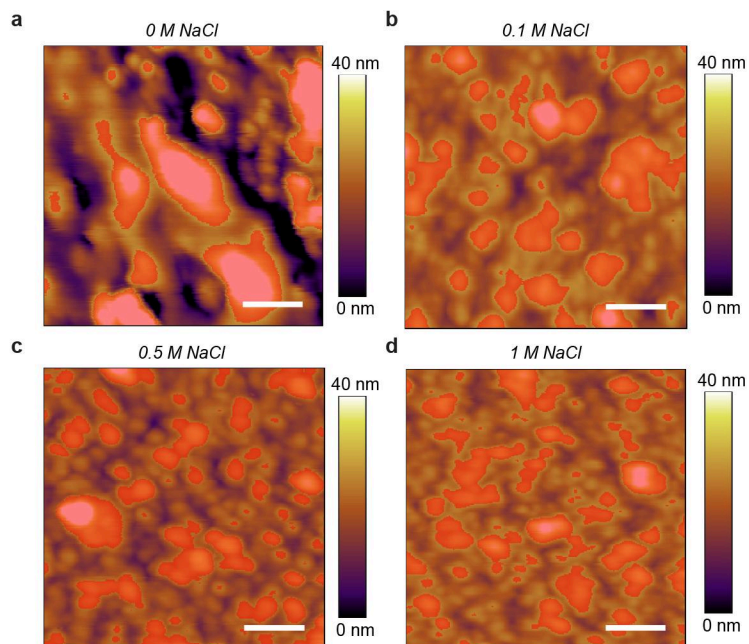
Supplementary Figure 1. Voltage-dependent absorbance change of PEDOT:PSS thin films at different wavelengths. Voltage-dependent absorbance changes of PEDOT:PSS films electropolymerized under different NaCl concentrations at commonly-used laser wavelengths: (a) 488 nm, (b) 510 nm, (c) 532 nm, (d) 658 nm, (e) 785 nm, and (f) 830 nm. The dashed vertical lines indicate 0 mV (vs. Ag/AgCl). A reverse in the voltage-dependent absorbance change trend is observed at higher laser wavelengths. Data for spin-coated PEDOT:PSS film from commercial suspension is included for comparison.



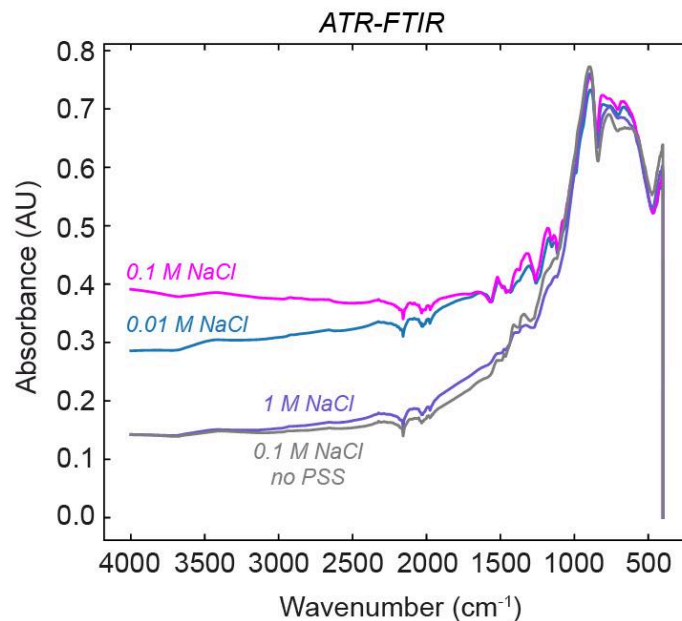
Supplementary Figure 2. Influence of pH, NaCl, and PSS molecular weight on the spectroelectrochemistry of electropolymerized PEDOT:PSS films. (a) π - π^* absorption peak wavelength as a function of electrolyte pH during electropolymerization. (b) Vis-NIR spectroelectrochemistry of PEDOT:Cl films electropolymerized with 0.1 M NaCl without PSS. (c) Vis-NIR spectroelectrochemistry of PEDOT:PSS films electropolymerized with 3.4 kDa and 15 kDa PSS (0 M NaCl). All measurements were performed from -900 mV to $+600$ mV versus Ag/AgCl in HEPES-buffered Tyrode's solution.



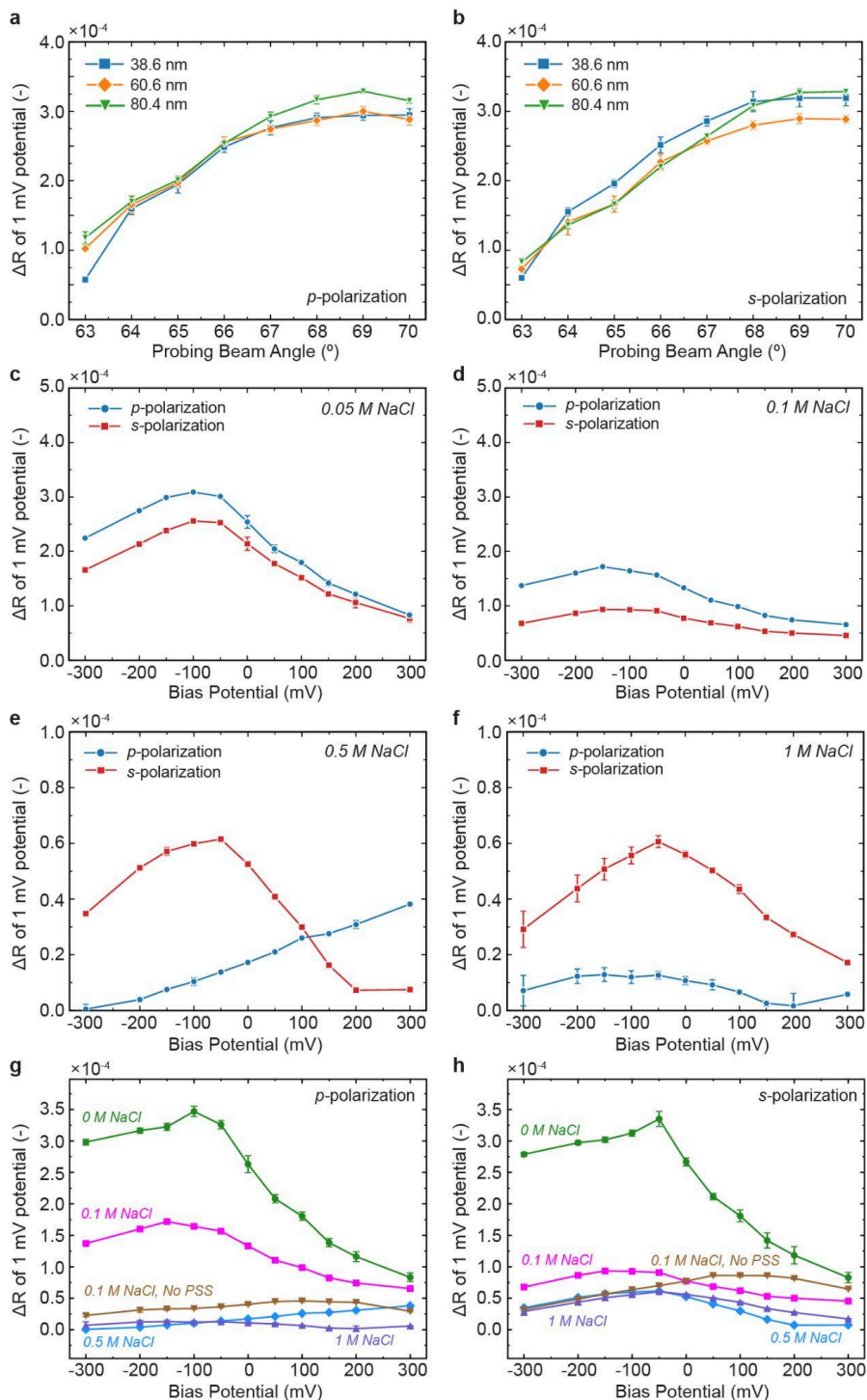
Supplementary Figure 3. Influence of ITO glass surface treatment on the spectroelectrochemistry of electropolymerized PEDOT:PSS films. (a) Atomic force microscopy (AFM) images of ITO glass substrates under different surface treatment conditions. Scale bar = 1 μm (top row) and 200 nm (bottom row). (b) Vis-NIR spectroelectrochemistry of PEDOT:PSS films electropolymerized on UV-Ozone-treated ITO glass with 0 M NaCl.



Supplementary Figure 4. Grain analysis on AFM images. A 75% rank was used as a fixed threshold for all samples. The area covered with red masks are suggested as “grains” in this analysis. PEDOT:PSS thin films electropolymerized with (a) 0 M, (b) 0.1 M, (c) 0.5 M, and (d) 1 M NaCl shows mean equivalent radii of 48.2 nm, 37.9 nm, 25.9 nm, and 26.8 nm, respectively.

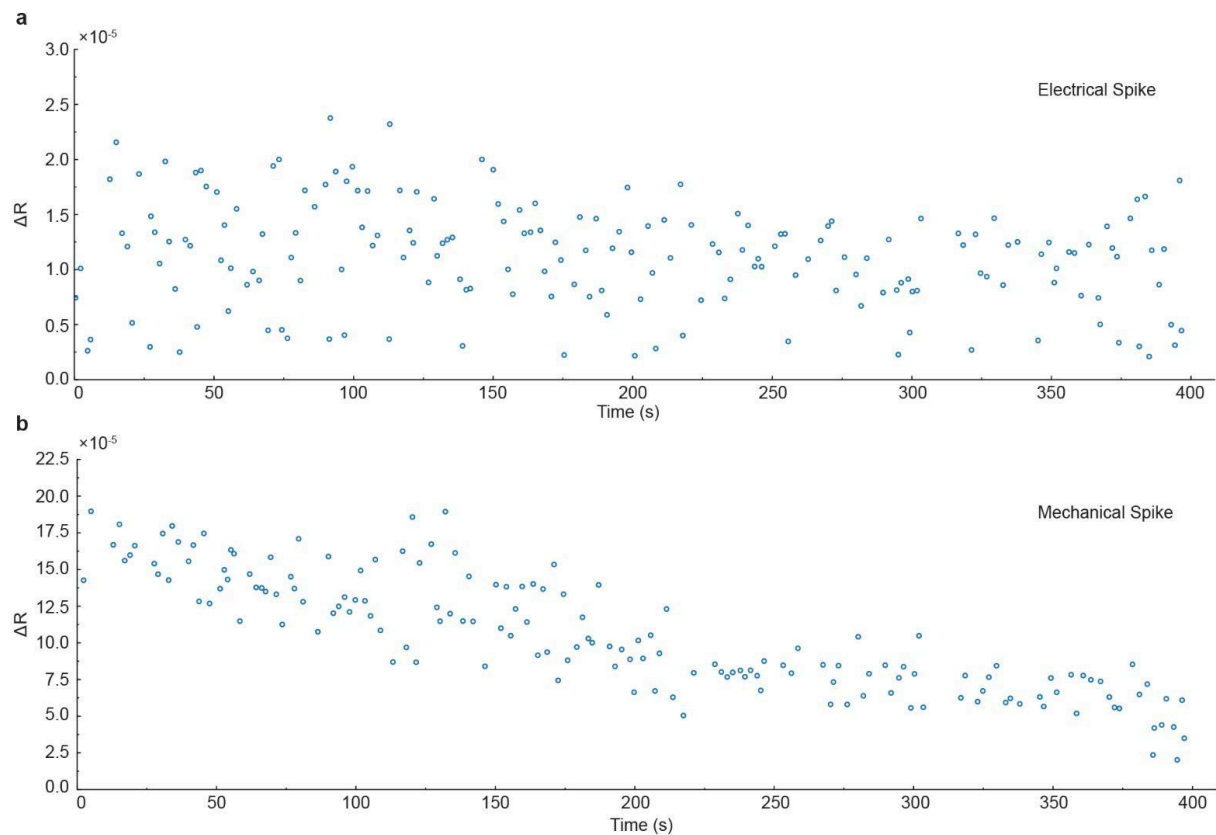


Supplementary Figure 5. ATR-FTIR spectra of PEDOT:PSS films electropolymerized under different NaCl concentrations. Characteristic bands are observed at $\sim 1520\text{ cm}^{-1}$, corresponding to C=C/C-C stretching of the thiophene ring. The region between $\sim 1100\text{-}1250\text{ cm}^{-1}$ is dominated by C-O-C stretching vibrations of the ethylenedioxy groups with contributions of -SO_3^- from PSS. Features around $\sim 970\text{-}1000\text{ cm}^{-1}$ are mainly attributed to C-S stretching modes of the thiophene ring¹. Qualitatively, 1 M NaCl and 0.1 M with no PSS conditions show largely reduced contributions from PSS. A baseline drift across the spectra is observed, arising from the wavelength-dependent infrared absorption of the underlying ITO glass substrate.



Supplementary Figure 6. Influence of probing beam incident angle, film thickness, and bias potential on ECORE signal in response to 1 mV, 1 Hz squarewave potential. Reflectance change (ΔR) as a function of probing beam incidence angle for PEDOT:PSS films with different thicknesses when measured using (a) p -polarized and (b) s -polarized light. Bias-potential dependence of ΔR measured under p -polarized and s -polarized light for PEDOT:PSS thin films electropolymerized with (c) 0.05 M, (d) 0.1 M, (e) 0.5 M, and (f) 1 M NaCl. ΔR of electropolymerized PEDOT:PSS and PEDOT:Cl films in

response to 1 mV, 1 Hz squarewave potential measured using (g) *p*-polarized and (h) *s*-polarized light under different bias potentials. Data are presented as mean \pm SD.



Supplementary Figure 7. Electrical and mechanical spike amplitudes of E10 chicken hearts recorded by ECORE with blebbistatin. Reflectance change, ΔR , as a function of time for (a) field potential spikes and (b) mechanical contraction spikes recorded from isolated E10 chicken hearts after 15 min incubation with blebbistatin. Each point represents a detected individual peak.

Supplementary Tables

<i>Sample</i>	PEDOT 2p 3/2	PEDOT 2p 1/2	PEDOT ⁺ 2p 3/2	PEDOT ⁺ 2p 1/2	PSS 2p 3/2	PSS 2p 1/2	R.S.F (S)	Cl ⁻ 2p 3/2	Cl ⁻ 2p 1/2	C-Cl 2p 3/2	C-Cl 2p 1/2	R.S.F (Cl)
0.1 M, no PSS	10627.6	5313.8	5098.7	2549.4	1650.4	825.2	1.677	1101.3	550.7	5709.6	2854.8	2.285
0.01 M	3133.3	1566.7	2958.4	1479.2	7430.0	3715.0	1.677	0.0	0.0	155.8	77.9	2.285
0.05 M	5143.0	2571.5	3899.0	1949.5	7872.1	3936.1	1.677	0.0	0.0	829.5	414.8	2.285
0.1 M	4092.3	2046.2	3395.4	1697.7	7786.7	3893.4	1.677	46.2	23.1	722.7	361.4	2.285
0.5 M	3803.6	1901.8	2778.5	1389.3	6838.1	3419.1	1.677	670.5	335.3	1275.2	637.6	2.285
1 M	4162.7	2081.4	3102.1	1551.1	9953.7	4976.9	1.677	0.0	0.0	1673.0	836.5	2.285

Supplementary Table 1. Fitted XPS peak areas of PEDOT:PSS films electropolymerized under different NaCl concentrations. Peak areas corresponding to PEDOT (2p), PEDOT⁺ (2p), PSS (2p), and Cl-related species (Cl⁻ 2p and C-Cl 2p) are listed for each sample, including a PSS-free control. Relative sensitivity factors (R.S.F.) for both elements used for quantification are also listed.

<i>Sample</i>	PSS/PEDOT	Cl/PEDOT	Cl/PSS
0.1 M, no PSS	0.105	0.318	3.029
0.01 M	1.220	0.019	0.015
0.05 M	0.871	0.067	0.077
0.1 M	1.040	0.075	0.072
0.5 M	1.039	0.217	0.209
1 M	1.370	0.169	0.123

Supplementary Table 2. Atomic ratios derived from XPS analysis of PEDOT:PSS films. Calculated ratios of PSS/PEDOT, Cl/PEDOT, and Cl/PSS for films electropolymerized under different NaCl concentrations, including a PSS-free control.

References

1. Sriprachuabwong, C. *et al.* Inkjet-printed graphene-PEDOT:PSS modified screen printed carbon electrode for biochemical sensing. *J. Mater. Chem.* **22**, 5478–5485 (2012).